Cureus
Part of SPRINGER NATURE

Open Access Original Article

Hard and Soft Tissue Factors Associated With Changes in the Buccal Corridor Area Ratio After Orthognathic Surgery

Review began 09/23/2026
Review ended 10/19/2026
Published 10/29/2026

© **Copyright** 2026
Nakamura et al. This is an open access article distributed under the terms of the Creative Commons Attribution License CC-BY 4.0., which permits unrestricted use, distribution, and reproduction in any medium, provided the original author and source are credited.

DOI: 10.7759/cureus.118776

Fumi Nakamura [1], Shinya Fuchida [2], Masahiro Takahashi [1], Rumi Matsumoto [1], Tetsutaro Yamaguchi [1]

1. Department of Orthodontics, School of Dentistry, Kanagawa Dental University, Yokosuka, JPN 2. Department of Education Planning, School of Dentistry, Kanagawa Dental University, Yokosuka, JPN

Corresponding author: Tetsutaro Yamaguchi, t.yamaguchi@kdu.ac.jp

Abstract

Background

The smile is a complex composite phenotype of hard tissue and perioral soft tissue characteristics. However, the factors associated with postoperative changes in the buccal corridor area ratio (BCAR), which standardizes the buccal corridor area relative to the total smile area enclosed by the inner borders of the lips, remain unclear. Therefore, this study explores the hard tissue and soft tissue factors associated with changes in the BCAR after orthognathic surgery.

Materials and methods

This single-center, retrospective, observational study evaluated 27 patients who underwent orthognathic surgery. Smile-related, skeletal, dental, and soft tissue parameters were measured using standardized frontal posed-smile photographs, lateral cephalometric radiographs, and cone-beam computed tomography (CBCT) images obtained immediately before surgery (T0) and approximately six months postoperatively (T1) to calculate the pre-to-postoperative changes (Δ= T1 − T0). Univariable correlation analysis and stepwise multiple linear regression analysis were performed, with the change in BCAR (ΔBCAR) designated as the dependent variable.

Results

ΔBCAR was 0.0030 ± 0.0170. In Model 1, the ΔSmile Index was significantly associated with ΔBCAR (B = 0.004, β = 0.539, p = 0.004; R^2 = 0.291, adjusted R^2 = 0.262). In the final stepwise regression model, the ΔSmile Index (B = 0.004, β = 0.510, p = 0.001) and change in point A-nasion-point B angle (ΔANB; B = -0.002, β = -0.479, p = 0.003) were selected as variables statistically associated with ΔBCAR (R^2 = 0.519, adjusted R^2 = 0.479). The variance inflation factor (VIF) for both variables was 1.004.

Conclusions

Postoperative changes in BCAR were statistically associated with changes in the Smile Index and ANB angle in this exploratory cohort. However, the association involving the Smile Index may partly reflect changes in vertical smile opening and their influence on TSA, the denominator of BCAR. These findings do not establish an independent biological relationship, causality, or individual predictive ability and should be interpreted as hypothesis-generating.

Categories: Plastic Surgery, Radiology, Dentistry
Keywords: buccal corridor area ratio, lateral cephalometry, orthognathic surgery, posed smile, smile index, soft tissue

Introduction

Although surgical orthodontic treatment for dentofacial deformities normalizes the relationship between the maxillomandibular bones and dentition, its major therapeutic goal is to establish stable occlusion and oral-masticatory functions along with a harmonious balance between frontal and profile facial esthetics and perioral soft tissues during active animation. Among these, the smile is a dynamic facial expression formed by the complex interaction of the teeth, gingiva, alveolar bone, jaws, lips, and perioral musculature; therefore, it cannot be adequately evaluated based on static resting profiles or lateral cephalometric radiographs alone. After orthognathic surgery, key esthetic parameters, including the smile line, smile arc, Smile Index, last visible posterior teeth, and buccal corridors, can vary dynamically depending on the patient's specific skeletal deformity [1]. Therefore, to thoroughly assess the success of surgical orthodontic treatment, frontal smile characteristics such as tooth-and-gingival exposure as well as perioral lip morphology during smiling should be evaluated as independent outcomes, along with skeletal correction and occlusal stability [2,3].

Smile morphology is dictated by the width and shape of the maxillary dentition; vertical position of the anterior teeth; occlusal plane; and anteroposterior, vertical, and transverse positions of the jaws, as well as the upper lip length, lip thickness, upper lip elevation, intercommissural width, and perioral muscle activity. Consequently, even with comparable hard tissue movements, postoperative smile changes are not uniform because of individual variations in soft tissue thickness, muscular function, postsurgical scarring, and dynamic facial expression patterns. Three-dimensional (3D) measurements have shown that soft tissue changes in the frontal view following orthognathic surgery can be quantified, increasingly revealing that skeletal displacement cannot be simply translated to soft tissue changes [4]. Furthermore, in patients with skeletal asymmetry, bilateral differences exist in both static morphological asymmetry and dynamic displacement of the oral commissures and lower lip during smiling [5].

These findings indicate that the postoperative smile is a complex composite phenotype of hard tissue and perioral soft tissue characteristics during smiling. The buccal corridor is the dark lateral negative space visible between the buccal surfaces of the maxillary posterior teeth and the oral commissures during a posed smile and represents a key indicator of horizontal smile fullness. In Japanese populations, the size of this space has been reported to significantly affect smile esthetics [6]. Conversely, comparisons between Japanese and Korean populations, evaluations between dental professionals and laypersons, and systematic reviews synthesizing lay esthetic evaluations suggest that the acceptable range of buccal corridors varies depending on contextual factors, such as the evaluator's professional specialty, cultural background, overall facial appearance, gingival display, and the smile arc [7-9]. Therefore, rather than evaluating buccal corridors based on a single "ideal value," they must be quantified as an integrated component of the entire smile framework, thereby distinguishing objective morphological changes from patient-perceived esthetic improvements.

Historically, the buccal corridors have often been evaluated as bilateral linear widths or as a ratio of the linear width to smile width. However, although linear measurements represent the horizontal extent of dark spaces, they do not adequately reflect the vertical morphology of oral commissures or the irregular boundaries along the last visible posterior teeth. The buccal corridor area ratio (BCAR), which standardizes the buccal corridor area (BCA) relative to the total smile area (TSA) enclosed by the inner vermilion borders of the lips, represents both the horizontal and vertical extents of the space as a single relative indicator, while mitigating the effects of photographic magnification. Yang et al. reported that the BCA and BCAR during a posed smile are associated with multiple hard tissue and soft tissue factors, including vertical facial soft tissue length, maxillary incisor exposure, and crown width [10]. However, because ratio indicators depend on changes in both the numerator and denominator, a change in the BCAR does not inherently imply a change in the BCA; this characteristic is crucial when interpreting postoperative changes.

Smiles can be broadly categorized as spontaneous smiles, which occur in response to emotions, and posed smiles, which are voluntarily expressed upon instruction. Although spontaneous smiles typically result in greater dental and gingival exposure and wider smile width, they are instantaneous, which makes the standardization of capture timing highly challenging [11,12]. In contrast, posed smiles are highly reproducible and are easily expressed repeatedly under identical conditions, making them suitable for longitudinal comparisons using clinical photographs. However, even with posed smiles, measurements can vary depending on the natural head position, occlusal state, camera distance, photographic magnification, lighting, instruction protocols, and image selection. Furthermore, a single static image fails to capture the velocity, trajectory, and bilateral differences throughout the cycle of smile expression. Therefore, the advantages of two-dimensional (2D) photographic evaluation lie in its clinical simplicity and applicability to existing clinical records rather than its capacity to fully represent dynamic perioral motion.

Orthognathic surgery alters the relative positional relationships among the dentition, lips, and oral commissures through multiple pathways. Maxillary advancement, superior repositioning, rotation, and correction of the occlusal plane can affect maxillary incisor and molar exposure, upper lip elevation, and the soft tissues of the alar base and perioral regions. Mandibular relocation influences lower facial height, lower lip support, and oral commissure movement, whereas correction of bilateral asymmetry can alter the symmetry of soft tissue movement during smiling. Changes in the upper lip and buccal corridors following Le Fort I osteotomy, as well as changes in the Smile Index and buccal corridors in skeletal Class III cases, have been previously reported [13,14]. Furthermore, investigations utilizing four-dimensional (4D) video stereophotogrammetry indicate that the magnitude and morphology of expressive facial movements, including smiles, can change after orthognathic surgery; however, these changes may not be fully explained by skeletal classification or surgical procedures alone [15].

A recent relatively large-scale study reported that the postoperative buccal corridor ratio varies in its direction of change depending on the skeletal pattern, increasing in Class II cases but decreasing in Class III cases [1]. This finding implies that when patients with Class II and Class III are collectively analyzed as a pooled sample, divergent directions of change can occur in individual patients, even if the overall mean change remains minimal. Furthermore, most previous studies have primarily focused on testing preoperative-to-postoperative differences, descriptive statistics for specific skeletal patterns, or simple correlations with individual jaw-relocation measurements. Consequently, the factors statistically associated with postoperative changes in BCAR, when simultaneously considering skeletal, dental, and perioral lip morphologies as well as the horizontal and vertical proportions of the smile, remain unclear.

Therefore, this study aimed to use standardized frontal posed smile photographs, lateral cephalometric radiographs, and cone-beam computed tomography (CBCT) images of patients who underwent orthognathic surgery to explore hard tissue factors and smile-related soft tissue factors statistically associated with changes in the BCAR from immediately before surgery to approximately six months postoperatively. The working hypothesis of this study was that changes in the BCAR are not solely explained by skeletal changes in jaw relationships but are also statistically associated with changes in soft tissue parameters representing the horizontal expansion and vertical opening of the smile.

Materials And Methods

Study design and ethical considerations

This study was designed as a non-interventional, single-center, retrospective observational study utilizing existing clinical records (including facial photographs) from Kanagawa Dental University Hospital. Rather than obtaining individual or comprehensive written consent, an opt-out consent methodology was implemented for research participation. Information sheets describing the study protocol and objectives were displayed at the orthodontic outpatient clinic of Kanagawa Dental University Hospital to inform eligible participants, thereby guaranteeing them the opportunity to decline the use of their records and information. This study was approved by the Kanagawa Dental University Research Ethics Review Committee (initial approval no. 1087, March 26, 2025; amendment approval no. 1234, September 17, 2026). The requirement for individual informed consent was waived, and an opt-out approach was used. Furthermore, facial photographs were processed and cropped to ensure patient anonymity; no patient photographs that could identify individuals were included in the manuscript. Individual written consent for the publication of patient photographs was not obtained, and both research use and public dissemination of these images were conducted in strict accordance with the aforementioned opt-out consent protocol. The manuscript was prepared and reported in accordance with the Strengthening the Reporting of Observational Studies in Epidemiology (STROBE) statement [16].

Participants

Patients who underwent surgical orthodontic treatment at Kanagawa Dental University Hospital between May 2024 and March 2026 and met the criteria were included as candidates. The inclusion criteria were as follows: (1) patients who underwent orthognathic surgery as part of surgical-orthodontic treatment after preoperative orthodontic treatment; (2) patients with standardized frontal posed-smile photographs, lateral cephalometric radiographs, and CBCT images obtained immediately before surgery (T0) and approximately six months postoperatively (T1); and (3) availability of complete records suitable for measurement at both time points. The following exclusion criteria were applied to eliminate potential confounding influences on lip dynamics: congenital craniofacial anomalies, syndromes, or cleft lip and palate; history of maxillofacial trauma or prior orthognathic surgery; soft tissue procedures directly affecting lip morphology during the evaluation period; cases in which relevant anatomical landmarks could not be reliably identified on lateral cephalometric radiographs or CBCT images; and cases in which accurate measurements were difficult owing to poor photographic or radiographic imaging quality.

All 28 patients who underwent orthognathic surgery at our institution during the study period had complete standardized posed-smile photographs, lateral cephalometric radiographs, and CBCT records at both T0 and T1 and were assessed for measurement eligibility. Of these, one patient was excluded because Point A could not be reliably identified on either lateral cephalometric or CBCT images, precluding reliable measurements of SNA and CBCT-derived ANB. The final cohort comprised 27 patients. Postoperative (T1) records were obtained at a mean follow-up interval of 6.01 ± 0.50 months (range: 5.2-7.4 months) after surgery. At T1, all patients were undergoing active postoperative orthodontic finishing and detailing with fixed appliances and intermaxillary elastics. None had undergone debonding. All 27 patients (7 males, 20 females; 14 single-jaw surgery cases, 13 bimaxillary orthognathic surgery cases, 14 skeletal Class II cases, and 13 skeletal Class III cases) were Japanese. Skeletal Class II and Class III cases were classified according to the baseline (T0) CBCT-derived ANB angle as follows: Skeletal Class II was defined as ANB > 4.0° (n = 14) and Skeletal Class III as ANB < 0.0° (n = 13). Bimaxillary surgery comprised maxillary Le Fort I osteotomy combined with mandibular bilateral sagittal split osteotomy (BSSO) (n = 13). All Le Fort I osteotomies were performed as single-piece procedures. No multi-piece segmented osteotomies or surgical transverse expansion or constriction were performed. Single-jaw surgery comprised mandibular BSSO alone (n = 14).

Standardized posed-smile photography

To acquire frontal posed-smile photographs at T0 and T1 using an identical method, each participant was positioned inside a cephalostat in the same manner as that during cephalometric radiography, with bilateral ear rods fitted into the external auditory meatus to stabilize the head. The head position was standardized such that the Frankfort horizontal (FH) plane was parallel to the floor, and the subjects were instructed to look straight ahead with their maxillary and mandibular molars in occlusion. The examiner instructed the participants to express a posed smile with complete bilateral expansion of their oral commissures, and the clearly expressed images were used for analysis. The distance between the subject and camera was set at 1.0 m; the camera height, photographic magnification, lighting, and background were strictly standardized and kept identical between T0 and T1. Photography was performed using a digital camera (EOS 800D; Canon

Inc., Tokyo, Japan) equipped with a DCC29-LV/GP3 lens (Sonic Technology Co., Ltd., Tokyo, Japan) with the following standardized settings: ring flash, shutter speed 1/125 s, aperture f/5.6, and ISO 100. ImageJ software version 1.54g (National Institutes of Health, Bethesda, MD, USA) was used for image analysis.

For image calibration, to serve as an invariant hard tissue reference scale unaffected by surgical procedures, the maximum mesiodistal crown width (mm) of the maxillary right central incisor on pre- (T0) and postoperative (T1) axial CBCT images was measured by a single examiner. To ensure measurement validity, the CBCT images were reoriented three-dimensionally along the long axis of the maxillary right central incisor, and the axial slice displaying the maximum crown width at the height of the contour was selected for measurement. Intra-examiner reliability was evaluated using an intraclass correlation coefficient (ICC) based on a two-way mixed-effects, single-measurement, absolute-agreement model (ICC(3,1)), with the rater treated as a fixed effect and the subjects treated as random effects; the Dahlberg random error (SDe) was calculated using Dahlberg's formula ($SDe = \sqrt{[\sum d^2/2N]}$), where d represents the difference between the first and second measurements and N represents the number of double measurements. Using the calculated individual measurement (mm) as a baseline and dividing it by the corresponding pixel width of the central incisor on the smile photograph, a unique millimeter conversion factor (calibration factor) was calculated for each smile photograph at T0 and T1, individually for each time point. By applying this individual conversion factor in ImageJ software (version 1.54g; National Institutes of Health, Bethesda, MD, USA), all 2D linear and areal measurements were converted into millimeters (mm) and square millimeters (mm^2), respectively.

Smile measurements

From the frontal posed-smile photographs at T0 and T1 (Figure *1*), the following parameters were measured (Figures *2*, *3*). (A) Lip-tooth relationship width (LTRW): the vertical distance from the lower border of the upper lip to the incisal edge of the maxillary central incisor; (B) upper lip elevation (UL elevation): calculated by subtracting the upper lip length during smiling (ULL_s) from the upper lip length at rest (ULL_r) (UL elevation = ULL_r − ULL_s), where the superimposed rest and smile photographs were evaluated by creating a template from each subject's rest photograph using Keynote software, version 14.4 (Apple Inc., Cupertino, CA, USA) and superimposing it onto the posed-smile photograph [13]. The at-rest photograph was captured immediately prior to the posed-smile photography at both T0 and T1 under identical standardized lighting, camera settings, distance, and natural head position (with the Frankfort horizontal plane parallel to the floor inside the cephalostat); (C-1) interlabial gap: linear distance between the stomion superius (Stms) and stomion inferius (Stoi) during smiling; (C-2) smile width: linear distance between the bilateral oral commissures (cheilion) during smiling; (D) buccal corridor area (BCA): total sum of the bilateral dark areas between the buccal surfaces of the last visible maxillary teeth and oral commissures; (E-3) upper lip area: area of the upper lip enclosed by the upper lip vermilion border; (E-4) lower lip area: area of the lower lip enclosed by the lower lip vermilion border; and (F) total smile area (TSA): area enclosed by the inner vermilion borders of the upper and lower lips. The BCAR was calculated as BCA/TSA. The Smile Index was calculated as the ratio of smile width to interlabial gap.

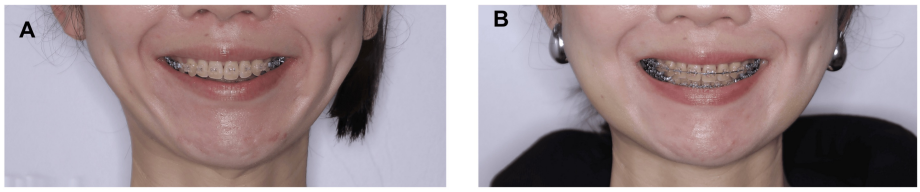


FIGURE 1: Preoperative and postoperative frontal posed-smile photographs.

(A) Immediately before orthognathic surgery (T0) in a patient with skeletal Class II malocclusion. (B) Approximately six months after orthognathic surgery (T1) in the same patient.

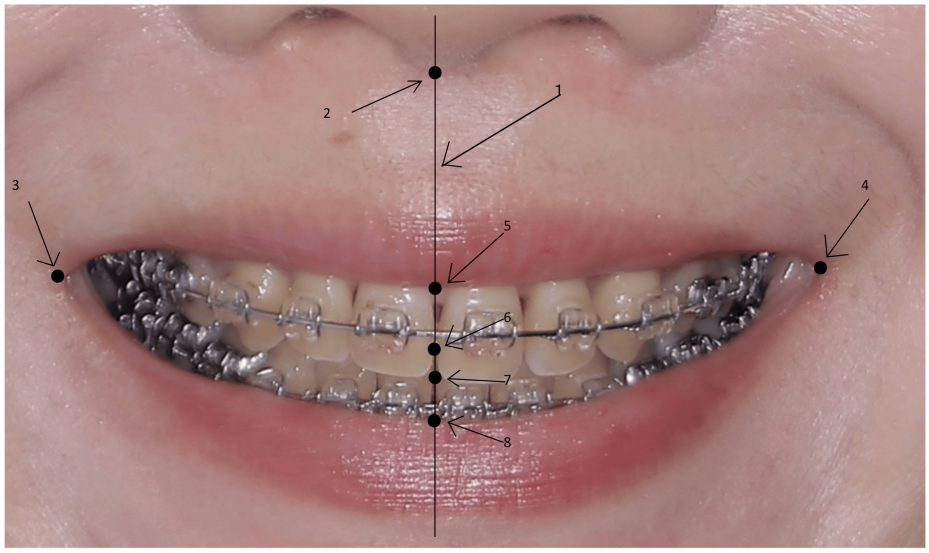


FIGURE 2: Landmarks for measuring variables.

(1) Facial midline, (2) subnasale (Sn), (3) right cheilion (Ch R), (4) left cheilion (Ch L), (5) stomion superius at smile (Stms_smile), (6) stomion superius at rest (Stms_rest), (7) incisor superius (Is), and (8) stomion inferius (Stoi).

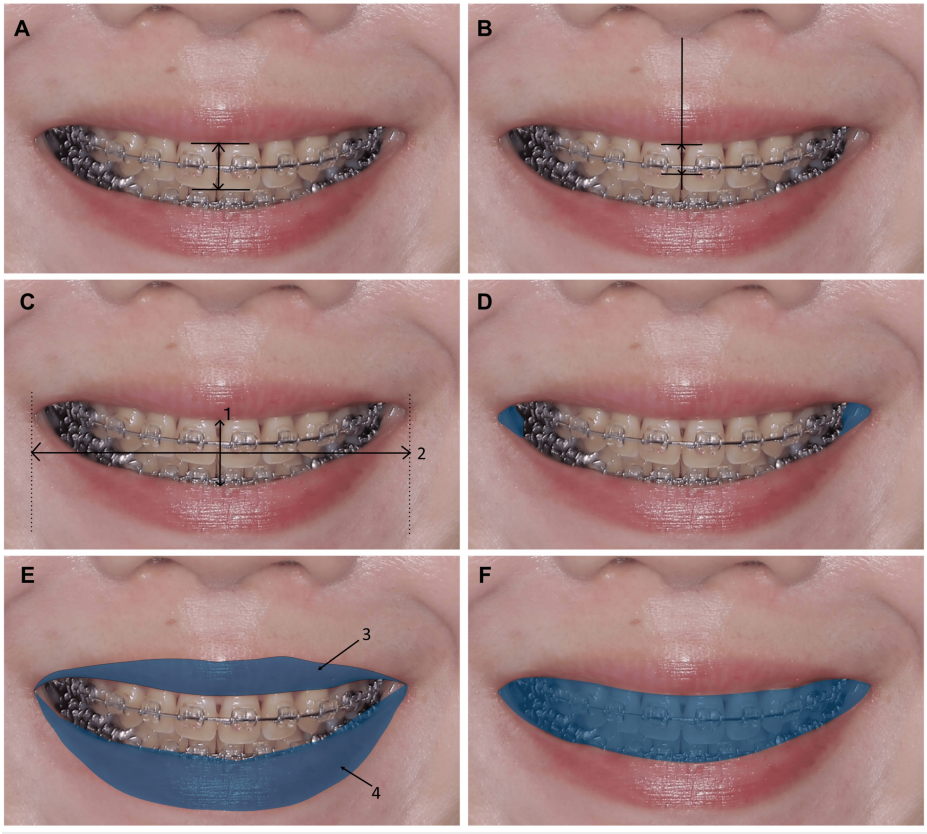


FIGURE 3: Guidelines for measuring variables.

(A) Lip-tooth relationship width (LTRW), measured from stomion superius at smile (Stms_smile) to incisor superius (Is). (B) Upper lip elevation, calculated as the distance from subnasale (Sn) to stomion superius at rest (Stms_rest) minus the distance from Sn to Stms_smile. (C) (1) Interlabial gap, measured from Stms_smile to stomion inferius (Stoi); (2) smile width, measured from the right cheilion (Ch R) to the left cheilion (Ch L). (D) Buccal corridor area (BCA). (E) (3) Upper lip area; (4) lower lip area. (F) Total smile area (TSA).

The symmetry ratios of the upper lip, lower lip, and left-to-right area were also measured as exploratory

parameters. The facial midline was defined as the vertical line passing through the midpoint of the bilateral inner canthi, perpendicular to the interpupillary line. The symmetry ratios of the upper lip area, lower lip area, and total smile area were calculated as respective ratios of the left-side area to the right-side area as bisected by the facial midline. All postoperative changes were calculated as Δ= T1 − T0, where a positive Δ-value indicated a postoperative increase and a negative Δ-value indicated a postoperative decrease.

Cephalometric and CBCT-derived measurements

Using lateral cephalometric radiographs at T0 and T1, a single examiner measured the skeletal parameters, including the sella-nasion-point A angle (SNA), sella-nasion-point B angle (SNB), and Frankfort-mandibular plane angle (FMA); dental parameters, including the upper central incisor-to-nasion-point A line angle and distance (U1-NA angle and U1-NA distance), lower central incisor-to-nasion-point B line angle and distance (L1-NB angle and L1-NB distance), interincisal angle, and lower incisor-mandibular plane angle (IMPA); and soft tissue and facial height parameters, including the subnasale-to-stomion superius distance (Sn-Stms) and anterior facial height (Figure *4*). To measure the ANB angle, a 3D image analysis software (Invivo6; Anatomage, San Jose, CA, USA) was used, and the angle was measured as a projection onto the midsagittal plane using three-dimensionally defined landmarks of the nasion (N), A-point (A), and B-point (B) (CBCT-derived ANB). This approach enhanced the 3D reproducibility in evaluating the anteroposterior skeletal relationship. CephaloMetrics AtoZ 20.0 (Yasunaga Computer System Co., Ltd., Fukui, Japan) was used for the cephalometric analysis. On CBCT images, the distance between the bilateral zygomatic points (zygomatic: the most medial point of the frontozygomatic suture in the external margin of the orbital rim on the left and right sides) and the ipsilateral maxillary first molar mesiobuccal cusp tip was measured. The value obtained by subtracting the left-side distance from the right-side distance was calculated as the transverse tilt (Figure *5*). CBCT imaging was performed using KaVo OP 3D Vision (KaVo Dental, Biberach, Germany) with the following exposure parameters: tube voltage 120 kV, tube current 5 mA, exposure time 17.8 seconds, and voxel size 0.3 mm.

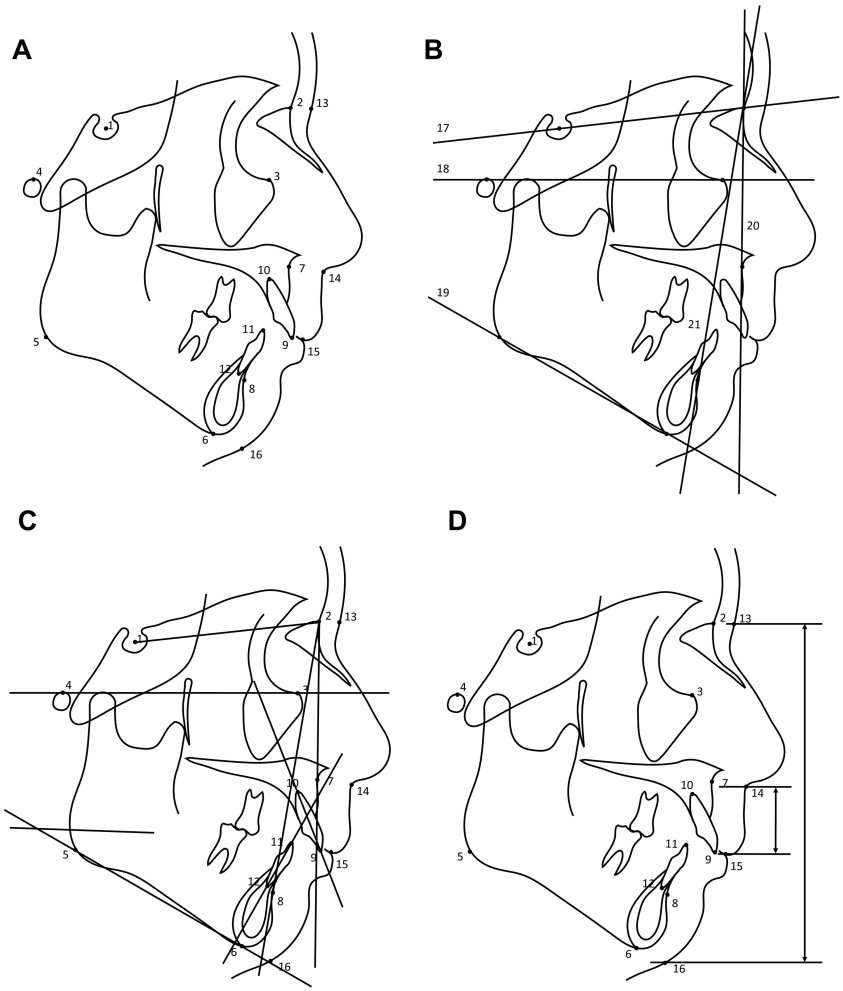


FIGURE 4: Cephalometric landmarks and reference lines.

(A) Cephalometric landmarks: 1, sella (S; center of the sella turcica); 2, nasion (N; most anterior point of the frontonasal suture); 3, orbitale (Or; most inferior point of the orbital margin); 4, porion (Po; most superior point of the external auditory meatus); 5, gonion (Go; constructed point at the mandibular angle that bisects the angle formed by the mandibular plane and ramus); 6. menton (Me; most inferior point on the mid-sagittal section of the mandibular symphysis); 7, point A (A; the deepest point on the anterior maxillary surface between the anterior nasal spine and maxillary incisor alveolus); 8, point B (B; the deepest point on the anterior surface of the mandibular symphysis between the infradentale and pogonion); 9, incisor superius (U1E; incisal edge of the most anterior maxillary central incisor); 10, root apex of the upper central incisor (U1A); 11, incisor inferius (L1E; incisal edge of the most anterior mandibular central incisor); 12, root apex of the lower central incisor (L1A); 13, soft tissue nasion (N'); 14, subnasale (Sn); 15, stomion superius (Stms); 16, soft tissue menton (Me').

(B) Reference lines: 17, sella to nasion (SN plane); 18, Frankfort horizontal plane (porion to orbitale); 19, mandibular plane (gonion to menton); 20 nasion to point A (NA line); 21, nasion to point B (NB line).

(C) Skeletal and dental measurements: a, SNA (degrees); b, SNB (degrees); c, FMA (degrees); d, U1-NA angle (U1 axis to NA line, degrees); e. U1-NA distance (U1E to NA line, mm); f, L1-NB angle (L1 axis to NB line, degrees); g, L1–NB distance (L1E to NB line, mm); h, interincisal angle (U1 axis to L1 axis, degrees); i, IMPA (degrees).

(D) Soft tissue measurements: a. Sn-Stms, mm; b. anterior facial height (N' to Me'), mm.

Image Credits: This cephalometric artwork was created by the authors.

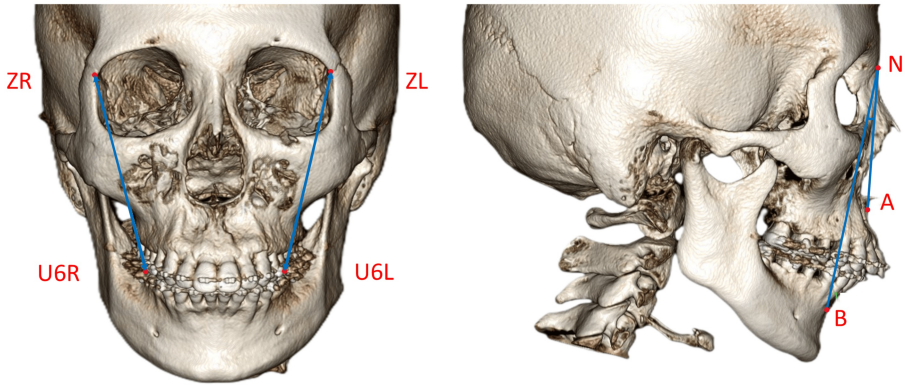


FIGURE 5: Cone-beam computed tomography (CBCT) images viewed with a Digital Imaging and Communications in Medicine (DICOM) viewer showing landmarks and measurements.

Landmarks: nasion (N), point A (A), point B (B), zygomatic point right (ZR), zygomatic point left (ZL), mesiobuccal cusp tip of the right maxillary first molar (U6R), and mesiobuccal cusp tip of the left maxillary first molar (U6L).

Measurements: 1, transverse tilt (the ZR-U6R distance minus the ZL-U6L distance, mm); 2, ANB angle (degrees).

Measurement error and reliability

To evaluate intra-examiner reproducibility, all 27 subjects were re-measured by the same examiner two weeks after the initial measurements. Random error was calculated using Dahlberg's formula ($\sqrt{[\Sigma d^2/2N]}$), and intra-examiner reliability was evaluated using a two-way mixed-effects model, single-measurement, absolute agreement ICC(3,1) with 95% confidence intervals (CIs), treating the rater as a fixed effect and the subjects as random effects. The model selection and reporting of ICCs followed the guidelines proposed by Koo and Li [17].

Statistical analysis

The normal distribution of continuous variables was assessed using the Shapiro-Wilk test, and preoperative to postoperative changes were summarized as mean ± standard deviation (SD). Univariable associations between ΔBCAR and each candidate variable were evaluated using Pearson's product-moment correlation coefficient (r). Additional exploratory Pearson correlation analyses were performed between raw ΔBCA and raw ΔTSA and the candidate variables to examine the components underlying the association between ΔSmile Index and ΔBCAR. Because the BCA is the numerator of the BCAR and is mathematically coupled with the dependent variable, it was excluded from the candidate independent variables for the regression models.

Subsequently, an exploratory multiple linear regression analysis was performed with ΔBCAR designated as the dependent variable. Variables exhibiting significant associations in the univariable analysis ($p < 0.05$) were selected as potential predictors. Exploratory multiple linear regression models were then constructed using a stepwise selection procedure, with a probability of F-to-enter of 0.05 and a probability of F-to-remove of 0.10. For each model, the unstandardized regression coefficient (B), standardized regression coefficient (β), coefficient of determination (R^2), adjusted R^2, p-values, and variance inflation factor (VIF) were calculated. Multicollinearity was evaluated using the VIF, and the underlying regression assumptions were verified. Linearity was assessed by visually inspecting the residual plots. For the final stepwise model, the normality of residuals, homoscedasticity, and influential observations were evaluated using the Shapiro-Wilk test, Breusch-Pagan test, and Cook's distance, respectively. Considering the sample size and number of candidate variables, the analysis was positioned as hypothesis-generating. An additional exploratory sensitivity analysis was performed using a fixed multiple linear regression model with ΔBCAR as the dependent variable. Baseline BCAR, ΔSmile Index, ΔANB (CBCT-derived), ΔLTRW, and ΔFMA were entered simultaneously using the enter method. Baseline BCAR was included to adjust for the preoperative outcome value, and ΔSmile Index and ΔANB were retained to reassess the principal associations identified in the primary analysis. ΔLTRW and ΔFMA were included based on their clinical relevance to incisor display and vertical skeletal morphology and previous findings relating upper incisor exposure and FMA to BCAR [10]. The previous incisor exposure measurement was obtained from lateral cephalograms with unstrained lips, whereas LTRW in this study was measured during posed smiling. The model was specified during manuscript revision, after the primary results were available, and no further significance-based variable selection was applied. Residual plots and the normal probability plot were visually examined, and VIFs and Cook's distances were assessed. Statistical analyses were performed using IBM SPSS Statistics for Windows, Version

29.0 (Released 2022; IBM Corp., Armonk, NY, USA), and a two-tailed $p < 0.05$ was considered statistically significant.

Results

Participants

The mean age of the 27 analyzed patients was 27.00 ± 10.33 years (range: 18-50 years). The postoperative (T1) records were obtained at a mean of 6.01 ± 0.50 months (range: 5.2-7.4 months) after surgery. Among the 14 patients with skeletal Class II, 4 underwent mandibular BSSO alone and 10 underwent Le Fort I osteotomy combined with BSSO. Among the 13 patients with skeletal Class III, 10 underwent mandibular BSSO alone and three underwent Le Fort I osteotomy combined with BSSO. The other demographic and clinical characteristics of the patients are shown in Table *1*.

Characteristic	Value
Number of participants	27
Age, years	27.00 ± 10.33 (18-50)
Male/female	7 (25.9%)/20 (74.1%)
Skeletal Class II/Class III	14 (51.9%)/13 (48.1%)
Single-jaw/bimaxillary surgery	14 (51.9%)/13 (48.1%)
Mandibular BSSO alone (single-jaw)	14 (51.9%)
Le Fort I + BSSO (bimaxillary)	13 (48.1%)
Class II: mandibular BSSO alone	4 (14.8%)
Class II: Le Fort I + BSSO	10 (37.0%)
Class III: mandibular BSSO alone	10 (37.0%)
Class III: Le Fort I + BSSO	3 (11.1%)
Interval from surgery to T1, months	6.01 ± 0.50 (5.2-7.4)

TABLE 1: Participant characteristics.

Data format: continuous variables are presented as mean ± standard deviation (SD), with ranges in parentheses; categorical variables are presented as counts and percentages (n (%)). Percentages were calculated based on the total sample of 27 participants.

BSSO: bilateral sagittal split osteotomy, T1: approximately six months postoperatively.

Measurement reliability

The intra-examiner reliability of the primary outcome, BCAR, demonstrated extremely high reproducibility, with an ICC(3,1) of 0.9982 (95% CI, 0.996-0.999; Dahlberg error, 0.001). Excellent reproducibility and measurement precision were confirmed across all evaluated skeletal, dental, soft tissue, and smile parameters. The Dahlberg random error (SDe) for angular parameters ranged from 0.127° (for the CBCT-derived ANB angle) to 0.421° (for the interincisal angle), with the corresponding ICC(3,1) values distributed within an extremely high range of 0.9940 to 0.9994. For linear parameters, the SDe remained within a narrow range, from 0.031 mm (for lip-tooth relationship width, LTRW) to 0.542 mm (for smile width), with the corresponding ICC values ranging from 0.9864 to 0.9998, indicating excellent intra-examiner reliability for all parameters. The SDe for area parameters ranged from 0.491 mm^2 to 0.918 mm^2 (for TSA), while the SDe for ratio/proportion parameters was small, ranging from 0.001 to 0.093, with all ICC values demonstrating absolute agreement exceeding 0.997. Furthermore, the mean clinical crown width of the maxillary right central incisor obtained from CBCT was 8.018 ± 0.540 mm (range: 6.81-8.85 mm). The ICC(3,1) was 0.9940 (95% CI: 0.990-1.000), indicating excellent consistency. The random error calculated using Dahlberg's formula was small (0.040 mm). The detailed reliability indices (ICC, 95% CIs, and Dahlberg error) for all variables are presented in Table *2*.

Variable	Unit	ICC (3,1)	95% CI lower	95% CI upper	Dahlberg error (SDe)	Interpretation

Skeletal characteristics						
Transverse tilt	mm	0.9885	0.975	0.995	0.329	Excellent
ANB	Degrees (°)	0.9994	0.999	1	0.127	Excellent
SNA	Degrees (°)	0.994	0.97	0.998	0.323	Excellent
SNB	Degrees (°)	0.9983	0.996	0.999	0.264	Excellent
FMA	Degrees (°)	0.9968	0.993	0.999	0.347	Excellent
Dental characteristics						
U1-NA angle	Degrees (°)	0.9988	0.997	0.999	0.288	Excellent
U1-NA distance	mm	0.9895	0.975	0.995	0.291	Excellent
L1-NB angle	Degrees (°)	0.9976	0.994	0.999	0.372	Excellent
L1-NB distance	mm	0.9913	0.981	0.996	0.302	Excellent
Interincisal angle (U1-L1)	Degrees (°)	0.9989	0.998	1	0.421	Excellent
IMPA angle	Degrees (°)	0.9981	0.996	0.999	0.371	Excellent
Soft tissue characteristics						
Sn-Stms distance (upper lip height)	mm	0.9891	0.976	0.995	0.376	Excellent
Anterior facial height (AFH)	mm	0.9984	0.996	0.999	0.355	Excellent
Interlabial gap	mm	0.9984	0.997	0.999	0.164	Excellent
Upper lip length at rest (ULL r)	mm	0.9916	0.982	0.996	0.303	Excellent
Upper lip length at smile (ULL s)	mm	0.9881	0.974	0.995	0.3	Excellent
Upper lip elevation	mm	0.9864	0.97	0.994	0.408	Excellent
Smile characteristics						
Smile width	mm	0.9909	0.98	0.996	0.542	Excellent
Lip tooth relationship width (LTRW)	mm	0.9998	1	1	0.031	Excellent
Upper lip total area	mm²	0.9998	1	1	0.624	Excellent
Lower lip total area	mm²	0.9998	0.999	1	0.848	Excellent
Total smile area (TSA)	mm²	1	1	1	0.918	Excellent
TSA symmetry ratio	Ratio	0.9998	1	1	0.003	Excellent
Buccal corridor area (BCA)	mm²	0.9987	0.997	0.999	0.491	Excellent
Buccal corridor area ratio (BCAR)	Ratio	0.9982	0.996	0.999	0.001	Excellent
Smile index	Ratio	0.9975	0.995	0.999	0.093	Excellent
Upper lip area symmetry ratio	Ratio	0.9979	0.995	0.999	0.011	Excellent
Lower lip area symmetry ratio	Ratio	0.9996	0.999	1	0.005	Excellent
CBCT reference standard/calibration anchor						
Maxillary right central incisor crown width	mm	0.994	0.99	1	0.04	Excellent

TABLE 2: Intra-examiner reliability indices, 95% confidence intervals, and Dahlberg errors for all evaluated parameters.

Reliability assessment: intra-examiner reliability was evaluated using a two-way mixed-effects model, single-measurement, absolute agreement ICC(3,1) with 95% CIs. Random error was calculated using Dahlberg's formula and is presented as SDe.

ICC: intraclass correlation coefficient, CI: confidence interval, SDe: Dahlberg random error, ANB: point A-nasion-point B angle, SNA: sella-nasion-point A angle, SNB: sella-nasion-point B angle, FMA: Frankfort-mandibular plane angle, U1: upper central incisor, NA: nasion-point A line, L1: lower central incisor, NB: nasion-point B line, IMPA: lower incisor-mandibular plane angle, Sn-Stms: subnasale-to-stomion superius distance, AFH: anterior facial height, ULL r: upper lip length at rest, ULL s: upper lip length at smile, LTRW: lip-tooth relationship width, TSA: total smile area, BCA: buccal corridor area, CBCT: cone-beam computed tomography.

Descriptive changes and univariable associations with ΔBCAR

The univariable associations between the changes in each variable and ΔBCAR are shown in Table *3*. ΔBCAR was 0.0030 ± 0.0170. ΔLTRW, ΔANB, Δtransverse tilt, Δinterlabial gap, ΔSmile Index, Δlower lip area, ΔSNB, and ΔL1-NB angle were associated with ΔBCAR ($p = 0.028$, 0.007, 0.039, 0.013, 0.004, 0.024, 0.007, and 0.006, respectively). These p-values represent exploratory results without correction for multiple comparisons and should be interpreted in conjunction with the correlation coefficients.

Variable	mean ± SD	r	p-value
ΔBCAR	0.0030 ± 0.0170	-	-
ΔLTRW (mm)	-1.01 ± 2.36	-0.424	0.028*
Age (years)	27.00 ± 10.33	0.137	0.496
ΔANB (CBCT-derived) (°)	1.17 ± 3.86	-0.509	0.007*
ΔTransverse tilt (mm)	0.19 ± 2.74	0.4	0.039*
ΔUpper lip elevation (mm)	-0.42 ± 3.10	-0.027	0.893
ΔInterlabial gap (mm)	-1.03 ± 3.53	-0.470	0.013*
ΔSmile width (mm)	-0.17 ± 4.22	0.137	0.497
ΔSmile Index	0.6563 ± 2.1219	0.539	0.004*
ΔUpper lip area (mm²)	-13.84 ± 42.33	0.253	0.202
ΔUpper lip area symmetry ratio	-0.0252 ± 0.1977	0.021	0.918
ΔLower lip area (mm²)	-17.85 ± 64.07	0.432	0.024*
ΔLower lip area symmetry ratio	-0.0352 ± 0.2158	-0.013	0.948
ΔTotal smile area (mm²)	-85.55 ± 176.80	-0.164	0.413
ΔTotal smile area symmetry ratio	-0.1043 ± 0.2553	-0.297	0.133
ΔSNA (°)	0.49 ± 1.40	-0.1	0.619
ΔSNB (°)	-0.83 ± 3.77	0.509	0.007*
ΔFMA (°)	0.54 ± 2.83	-0.271	0.171
ΔU1-NA (°)	-0.68 ± 2.07	0.064	0.752
ΔU1-NA (mm)	-0.16 ± 1.28	0.103	0.611
ΔL1-NB (°)	-1.19 ± 4.68	0.516	0.006*
ΔL1-NB (mm)	-0.74 ± 1.99	0.241	0.225
ΔInterincisal angle (°)	0.56 ± 4.17	-0.114	0.573
ΔIMPA (°)	-0.89 ± 3.49	0.364	0.062
ΔSn-Stms (mm)	1.05 ± 3.13	0.142	0.481
ΔAnterior facial height (mm)	1.41 ± 2.25	-0.015	0.941

TABLE 3: Descriptive statistics and univariable associations with ΔBCAR.

Values are presented as mean ± standard deviation (SD). Except for age, values represent changes (Δ) from immediately before surgery (T0) to approximately six months postoperatively (T1), calculated as Δ = T1 − T0.

Statistical analysis: univariable associations with ΔBCAR were evaluated using Pearson's correlation coefficient (r). A two-tailed p-value < 0.05 was considered statistically significant. An asterisk (*) indicates statistical significance (p < 0.05).

Δ: change from T0 to T1, T0: immediately before surgery, T1: approximately six months postoperatively, BCAR: buccal corridor area ratio, LTRW: lip-tooth relationship width, ANB: point A-nasion-point B angle, CBCT: cone-beam computed tomography, SNA: sella-nasion-point A angle, SNB: sella-nasion-point B angle, FMA: Frankfort-mandibular plane angle, U1: upper central incisor, NA: nasion-point A line, L1: lower central incisor, NB: nasion-point B line, IMPA: lower incisor-mandibular plane angle, Sn: subnasale, Stms: stomion superius.

The additional correlations with raw ΔBCA and raw ΔTSA are presented in Table *4* and Table *5*, respectively. ΔInterlabial gap was positively correlated with ΔTSA (r = 0.668, P < 0.001). ΔSmile Index was negatively correlated with ΔTSA (r = -0.619, p = 0.001), whereas its correlation with ΔBCA was not statistically significant (r = 0.177, p = 0.376). These additional analyses were exploratory, and p-values were not adjusted for multiple comparisons.

Variable	mean ± SD	r	p-value
ΔBCA (mm²)	-0.83 ± 11.98	-	-
ΔLTRW (mm)	-1.01 ± 2.36	-0.018	0.927
Age (years)	27.00 ± 10.33	0.215	0.283
ΔANB (CBCT-derived) (°)	1.17 ± 3.86	-0.488	0.01
ΔTransverse tilt (mm)	0.19 ± 2.74	0.223	0.263
ΔUpper lip elevation (mm)	-0.42 ± 3.10	0.041	0.84
ΔInterlabial gap (mm)	-1.03 ± 3.53	-0.106	0.597
ΔSmile width (mm)	-0.17 ± 4.22	0.495	0.009
ΔSmile Index	0.6563 ± 2.1219	0.177	0.376
ΔUpper lip area (mm²)	-13.84 ± 42.33	0.254	0.201
ΔUpper lip area symmetry ratio	-0.0252 ± 0.1977	0.017	0.934
ΔLower lip area (mm²)	-17.85 ± 64.07	0.358	0.067
ΔLower lip area symmetry ratio	-0.0352 ± 0.2158	-0.216	0.28
ΔTotal smile area (mm²)	-85.55 ± 176.80	0.328	0.095
ΔTotal smile area symmetry ratio	-0.1043 ± 0.2553	0.189	0.346
ΔSNA (°)	0.49 ± 1.40	-0.21	0.293
ΔSNB (°)	-0.83 ± 3.77	0.395	0.041
ΔFMA (°)	0.54 ± 2.83	-0.31	0.115
ΔU1-NA (°)	-0.68 ± 2.07	0.172	0.392
ΔU1-NA (mm)	-0.16 ± 1.28	0.230	0.248
ΔL1-NB (°)	-1.19 ± 4.68	0.393	0.042
ΔL1-NB (mm)	-0.74 ± 1.99	0.216	0.28
ΔInterincisal angle (°)	0.56 ± 4.17	-0.095	0.637
ΔIMPA (°)	-0.89 ± 3.49	0.353	0.071
ΔSn-Stms (mm)	1.05 ± 3.13	0.16	0.425
ΔAnterior facial height (mm)	1.41 ± 2.25	-0.055	0.784

TABLE 4: Descriptive statistics and exploratory correlations with changes in buccal corridor area (ΔBCA).

Values are presented as mean ± standard deviation (SD) for 27 patients. Except for age, all values represent changes from immediately before surgery (T0) to approximately six months postoperatively (T1), calculated as Δ = T1 − T0. Pearson's correlation coefficients (r) and two-tailed p-values describe the associations of each variable with raw ΔBCA. p-values are exploratory and were not adjusted for multiple comparisons. Dashes indicate entries that are not applicable.

Δ: change from T0 to T1, BCA: buccal corridor area, TSA: total smile area, LTRW: lip-tooth relationship width, ANB: point A-nasion-point B angle, CBCT: cone-beam computed tomography, SNA: sella-nasion-point A angle, SNB: sella-nasion-point B angle, FMA: Frankfort-mandibular plane angle, U1: upper central incisor, L1: lower central incisor, NA: nasion-point A line, NB: nasion-point B line, IMPA: lower incisor-mandibular plane angle, Sn: subnasale, Stms: stomion superius.

Variable	mean ± SD	r	p-value
ΔTotal smile area (mm²)	-85.55 ± 176.80	-	-
ΔLTRW (mm)	-1.01 ± 2.36	0.596	0.001
Age (years)	27.00 ± 10.33	0.096	0.633
ΔANB (CBCT-derived) (°)	1.17 ± 3.86	-0.21	0.293
ΔTransverse tilt (mm)	0.19 ± 2.74	-0.112	0.578
ΔUpper lip elevation (mm)	-0.42 ± 3.10	-0.039	0.848
ΔInterlabial gap (mm)	-1.03 ± 3.53	0.668	<0.001
ΔSmile width (mm)	-0.17 ± 4.22	0.390	0.045
ΔSmile Index	0.6563 ± 2.1219	-0.619	0.001
ΔUpper lip area (mm²)	-13.84 ± 42.33	0.227	0.254
ΔUpper lip area symmetry ratio	-0.0252 ± 0.1977	0.055	0.785
ΔLower lip area (mm²)	-17.85 ± 64.07	-0.274	0.167
ΔLower lip area symmetry ratio	-0.0352 ± 0.2158	-0.220	0.269
ΔTotal smile area symmetry ratio	-0.1043 ± 0.2553	0.925	<0.001
ΔSNA (°)	0.49 ± 1.40	0.081	0.688
ΔSNB (°)	-0.83 ± 3.77	0.152	0.448
ΔFMA (°)	0.54 ± 2.83	-0.273	0.168
ΔU1-NA (°)	-0.68 ± 2.07	-0.102	0.614
ΔU1-NA (mm)	-0.16 ± 1.28	0.044	0.827
ΔL1-NB (°)	-1.19 ± 4.68	-0.045	0.822
ΔL1-NB (mm)	-0.74 ± 1.99	0.097	0.63
ΔInterincisal angle (°)	0.56 ± 4.17	0.212	0.288
ΔIMPA (°)	-0.89 ± 3.49	-0.007	0.973
ΔSn-Stms (mm)	1.05 ± 3.13	0.023	0.908
ΔAnterior facial height (mm)	1.41 ± 2.25	-0.094	0.641

TABLE 5: Descriptive statistics and exploratory correlations with changes in total smile area (ΔTSA).

Values are presented as mean ± standard deviation (SD) for 27 patients. Except for age, all values represent changes from immediately before surgery (T0) to approximately six months postoperatively (T1), calculated as Δ = T1 − T0. Pearson's correlation coefficients (r) and two-tailed p-values describe the associations of each variable with raw ΔTSA. p-values are exploratory and were not adjusted for multiple comparisons. Dashes indicate entries that are not applicable.

Δ: change from T0 to T1, TSA: total smile area, LTRW: lip-tooth relationship width, ANB: point A-nasion-point B angle, CBCT: cone-beam computed tomography, SNA: sella-nasion-point A angle, SNB: sella-nasion-point B angle, FMA: Frankfort-mandibular plane angle, U1: upper central incisor, L1: lower central incisor, NA: nasion-point A line, NB: nasion-point B line, IMPA: lower incisor-mandibular plane angle, Sn: subnasale, Stms: stomion superius.

Multiple regression analysis

The results of multiple linear regression analysis with ΔBCAR designated as the dependent variable are presented in Table 6. In Model 1, the ΔSmile Index was extracted as an associated factor, the model R^2 was 0.291, and adjusted R^2 was 0.262 ($F(1, 25) = 10.24$, $P = 0.004$). In Model 2 (the final model), ΔSmile Index and ΔANB (CBCT-derived) were identified as variables statistically associated with ΔBCAR. The model R^2 was 0.519, and the adjusted R^2 was 0.479 ($F(2, 24) = 12.95$, $p < 0.001$). The VIF was 1.004 for each independent variable. In the residual analysis of the final model, residual plots did not suggest substantial departures

from linearity. The normality of the residuals was confirmed using the Shapiro-Wilk test (p = 0.874), and homoscedasticity was verified using the Breusch-Pagan test (p = 0.560), indicating no violations of regression assumptions. Furthermore, the maximum Cook's distance was 0.297.

Model/variable	B	β	P	95% CI for B	VIF	R^2	Adj. R^2
Model 1: ΔSmile Index	0.004	0.539	0.004	0.00154 to 0.00709	1	0.291	0.262
Model 2: ΔSmile Index	0.004	0.51	0.001	0.00174 to 0.00642	1.004	0.519	0.479
Model 2: ΔANB	-0.002	-0.479	0.003	-0.00339 to -0.00082	1.004		

TABLE 6: Exploratory multiple linear regression models for ΔBCAR.

Values are presented as unstandardized regression coefficients (B), standardized regression coefficients (β), 95% CIs for B, variance inflation factors (VIFs), coefficients of determination (R^2), and adjusted coefficients of determination (adjusted R^2). The change in the buccal corridor area ratio (ΔBCAR) was designated as the dependent variable. Exploratory multiple linear regression analysis was performed using a stepwise selection method. The changes in BCAR and Smile Index are unitless, whereas the change in the point A-nasion-point B angle (ΔANB) is expressed in degrees (°). A two-tailed p-value < 0.05 was considered statistically significant.

B: unstandardized regression coefficient, β: standardized regression coefficient, CI: confidence interval, VIF: variance inflation factor, Δ: change from immediately before surgery to approximately six months postoperatively, BCAR: buccal corridor area ratio, ANB: point A-nasion-point B angle.

Sensitivity analysis

All 27 patients were included in the baseline-adjusted sensitivity analysis (Table 7). The mean baseline BCAR was 0.0210 ± 0.0120 (mean ± SD). ΔSmile Index remained positively associated with ΔBCAR (B = 0.00292, β = 0.366, 95% CI: 0.00034-0.00551, p = 0.029), whereas ΔANB remained negatively associated with ΔBCAR (B = -0.00191, β = −0.435, 95% CI: -0.00330 to -0.00051, p = 0.010). Baseline BCAR, ΔLTRW, and ΔFMA were not statistically significant in this model. The model had an R^2 of 0.601 and an adjusted R^2 of 0.506 ($F(5, 21) = 6.335$, $p < 0.001$). VIFs ranged from 1.230 to 1.529, and the maximum Cook's distance was 0.214. The directions of the associations involving ΔSmile Index and ΔANB were consistent with those in the primary analysis.

Variable	B	β	p-value	95% CI for B	VIF	R^2	Adj. R^2
Baseline BCAR	-0.20713	-0.146	0.389	-0.69642 to 0.28217	1.452	0.601	0.506
ΔSmile Index	0.00292	0.366	0.029	0.00034 to 0.00551	1.276		
ΔANB	-0.00191	-0.435	0.01	-0.00330 to -0.00051	1.230		
ΔLTRW	-0.00191	-0.265	0.108	-0.00427 to 0.00046	1.314		
ΔFMA	-0.00013	-0.021	0.901	-0.00225 to 0.00200	1.529		

TABLE 7: Exploratory baseline-adjusted sensitivity analysis for ΔBCAR.

Values are presented as unstandardized regression coefficients (B), standardized regression coefficients (β), two-tailed p-values, 95% CIs for B, and variance inflation factors (VIFs). The dependent variable was ΔBCAR. Baseline BCAR, ΔSmile Index, ΔANB (CBCT-derived), ΔLTRW, and ΔFMA were entered simultaneously using the enter method. All 27 patients were included.

$R^2 = 0.601$; adjusted $R^2 = 0.506$; $F(5, 21) = 6.335$; $p < 0.001$. R^2 and adjusted R^2 refer to the entire model. Baseline BCAR, ΔBCAR, and ΔSmile Index are unitless; ΔLTRW is expressed in millimeters, and ΔANB and ΔFMA are expressed in degrees. p-values are exploratory and were not adjusted for multiple comparisons.

BCAR: buccal corridor area ratio, ANB: point A-nasion-point B angle, CBCT: cone-beam computed tomography, LTRW: lip-tooth relationship width, FMA: Frankfort-mandibular plane angle, Δ: change from immediately before surgery (T0) to approximately six months postoperatively (T1).

Discussion

Principal findings

In this study, the ΔSmile Index and ΔANB (CBCT-derived) remained in the final multiple linear regression model for ΔBCAR after orthognathic surgery. The model accounted for 51.9% of the variance in ΔBCAR, with an adjusted coefficient of determination (adjusted R^2) of 47.9%. Based on the VIF of 1.004, no obvious linear

multicollinearity was present between the two independent variables, the ΔSmile Index and ΔANB.

However, the association involving ΔSmile Index requires cautious interpretation. Changes in the interlabial gap were closely related to changes in TSA and may influence both the Smile Index and BCAR through their geometrically related components. Therefore, the regression result does not establish that Smile Index changes have a biological association with BCAR changes independent of vertical smile opening.

In the sensitivity analysis incorporating baseline BCAR, ΔLTRW, and ΔFMA, the positive association of ΔSmile Index and the negative association of ΔANB with ΔBCAR remained statistically significant. The standardized coefficient for ΔSmile Index was smaller than in the primary model (0.366 versus 0.510), whereas the coefficient for ΔANB changed less substantially (-0.435 versus -0.479). These findings indicate that the principal associations were retained under this alternative model specification. Because three explanatory variables were added simultaneously, the changes in coefficients cannot be attributed specifically to baseline adjustment. Neither ΔLTRW nor ΔFMA showed a statistically significant conditional association with ΔBCAR; however, this should not be interpreted as evidence that incisor display or vertical skeletal morphology is irrelevant to buccal corridor characteristics.

However, the value of $R^2 = 0.519$ cannot be interpreted as indicating a high predictive performance of the model. The regression coefficients and R^2 in this study are apparent values calculated from the same 27 cases used for variable selection, which may have been optimistically biased owing to the inclusion of a stepwise selection process. Furthermore, the two associated variables were not experimentally manipulated as "causes" but were indicators that changed simultaneously because of surgery, postoperative orthodontic treatment, perioral muscle activity, and smile expression intensity during photography. Therefore, this study only demonstrated that the ΔSmile Index and ΔANB were statistically associated with ΔBCAR within the range of observed changes; it does not imply that the BCAR of individual patients can be predicted, nor does it suggest that manipulating either variable may directly improve the BCAR.

Smile index and smile-related soft tissue morphology

The Smile Index is calculated as smile width divided by the interlabial gap, whereas BCAR is calculated as BCA divided by TSA. In the additional analyses, ΔInterlabial gap was positively correlated with ΔTSA ($r = 0.668$, $p < 0.001$), indicating that changes in TSA were closely related to changes in the vertical opening of the mouth. ΔSmile Index was negatively correlated with ΔTSA ($r = -0.619$, $p = 0.001$), whereas its correlation with ΔBCA was not statistically significant ($r = 0.177$, $p = 0.376$).

These findings suggest that the association between ΔSmile Index and ΔBCAR may partly reflect changes in vertical smile opening and their influence on the denominator of BCAR. For example, if BCA and smile width remain unchanged, a reduction in the interlabial gap accompanied by a reduction in TSA would increase both the Smile Index and BCAR. Thus, the retention of ΔSmile Index in the multiple regression model may partly reflect this geometric relationship rather than a biological association independent of vertical smile opening. However, the additional correlations do not establish that this mechanism fully accounts for the observed association or quantify its contribution. The low VIF indicates little linear collinearity between ΔSmile Index and ΔANB, but does not exclude this geometric relationship between ΔSmile Index and ΔBCAR.

Furthermore, although posed smiles are highly suitable for longitudinal comparisons, a single static image does not capture the dynamic velocity, kinetic trajectory, and bilateral asymmetry throughout the cycle of smile expression. In patients with skeletal asymmetry, 3D dynamic analysis has demonstrated that displacement of the oral commissures and lower lip differs between the deviated and non-deviated sides [5]. Comparisons before and after orthognathic surgery using 4D video stereophotogrammetry have also indicated that the magnitude, morphological changes, and symmetry of perioral motion during smiling can be altered postoperatively [15]. Therefore, the Smile Index in this study can be reasonably positioned, not as a direct measure of dynamic function, but as a standardized, single-point morphological surrogate of dynamic facial expression.

Sagittal jaw relationship and heterogeneity of surgical patterns

The ΔANB was negatively associated with ΔBCAR; holding other independent variables constant, for each 1° increase in the ANB angle, the BCAR was associated with a 0.002 decrease on the ratio scale utilized in this analysis. The ANB angle is an indicator of the anteroposterior jaw relationship based on points N, A, and B. This parameter was calculated by projecting three-dimensionally defined landmarks on the CBCT images onto the mid-sagittal plane (CBCT-derived ANB). Consequently, different surgical modifications, such as maxillary advancement, mandibular relocation, bimaxillary surgery, and jaw rotation, can produce the same ΔANB. Furthermore, because it is inherently influenced by the position of the nasion and rotational movements of the jaws, it does not directly represent actual 3D skeletal displacement. Therefore, the association between ΔANB and ΔBCAR does not directly indicate that a specific surgical skeletal movement drives the alteration in buccal corridors. Actual 3D surgical displacement was not quantified in this study. Therefore, we could not determine which specific directions or magnitudes of maxillary and mandibular movement contributed to the observed association between ΔANB and ΔBCAR.

Furthermore, the patient population in this investigation comprised a mixture of skeletal Class II and Class III patterns as well as single-jaw and bimaxillary orthognathic surgeries. Bimaxillary surgery was performed in 10 of 14 Class II patients and three of 13 Class III patients, indicating an uneven distribution of surgical procedures across skeletal classes. This imbalance may have influenced the pooled associations. In skeletal Class III cases, an increase in the ANB angle typically represents a therapeutic improvement in the anteroposterior jaw relationship, whereas in skeletal Class II cases, the direction of the change and its clinical significance differ. Zhong et al. reported that the postoperative buccal corridor ratio increased in patients with Class II but decreased in patients with Class III after orthognathic surgery [1]. Therefore, the negative regression coefficient obtained in this study, which pooled all skeletal patterns, may not represent a unidirectional biological response common to all cases but rather a pooled-sample average association reflecting the distribution of skeletal patterns, surgical procedures, and directions of skeletal movement. If effect modification is indeed affected by the skeletal pattern, the coefficient of the overall model may differ from the true associations within each individual skeletal pattern.

Following Le Fort I osteotomy, the vertical position of the maxilla, upper lip dynamics, last visible teeth, and buccal corridors can undergo significant alterations. Dilaver et al. reported an association between the extent of superior maxillary repositioning and certain buccal corridor parameters; however, not all jaw displacement measurements were consistently associated [13]. Chiang et al. evaluated patients with skeletal Class III and demonstrated that the Smile Index, interlabial gap, buccal corridors, and lip area changed postoperatively [14]. Additionally, 3D frontal analysis can quantify the soft tissue changes following bimaxillary surgery in both the horizontal and vertical directions, even though hard and soft tissue responses differ across distinct facial regions [4]. Even after synthesizing these findings, the ANB angle alone is insufficient to fully explain BCAR; therefore, the three-dimensional maxillary movement, occlusal plane rotation, dental arch width, last visible teeth, and oral commissure dynamics need to be simultaneously evaluated.

Interpretation of an area-based ratio

Evaluating the BCAR as a two-dimensional area standardized by the TSA represents a key methodological advantage of this study, distinguishing it from prior investigations that primarily evaluated simple linear widths [8,9]. The primary benefit of evaluating the BCAR is its capacity to represent the space as a relative proportion of the entire smile, thereby incorporating the vertical expansion of irregular dark areas that are inherently difficult to capture using linear widths alone. Even when photographs cannot be proportionally calibrated, the area ratio within the same image remains theoretically less susceptible to the effects of photographic magnification. This characteristic offers a major practical advantage for longitudinal and pre-to-postoperative comparisons using standard clinical photographs. Conversely, as the BCAR is mathematically formulated as BCA/TSA, a decrease in the ratio can result from a decrease in the BCA, an increase in the TSA, or both. As clinically distinct morphological variations can yield identical BCAR, this indicator alone cannot differentiate the mechanism underlying dynamic change.

For the same reason, treating BCA as an independent variable when evaluating BCAR induces a part-whole correlation, wherein the numerator of the dependent variable is reused as a predictor. Although excluding BCA from the regression candidates in this study was appropriate and statistically sound, it did not completely resolve all the methodological issues inherent to ratio indicators. Other smile parameters, including the smile width and interlabial gap, which dictate the TSA (the denominator of the BCAR), also share common morphological components with the dependent variable. In the present study, the additional analyses of raw ΔBCA and raw ΔTSA provide information on the components underlying BCAR, but do not distinguish geometric coupling from an independent biological response. Future studies should further examine bilateral BCA, the last visible posterior teeth, smile width, and interlabial gap to clarify the mechanisms underlying these changes.

In the present study, the mean ΔBCAR was 0.0030, which is relatively small as a pooled-sample average. However, this minimal change may be attributed to the directions of change offsetting between patients with Class II and Class III, substantial individual variation, or the fact that BCAR was analyzed on a ratio scale ranging from 0 to 1. Although existing esthetic evaluation studies indicate an acceptable range of buccal corridors, these perception thresholds depend heavily on image-manipulation methodologies, evaluators, and other confounding smile elements [9]. As this study was strictly a morphometric investigation and did not include esthetic evaluations by patients or lay evaluators, these statistical associations should not be directly equated with improvements in smile esthetics.

Relation to previous studies

The results of this study are highly consistent with those of previous reports, indicating that the postoperative smile changes after orthognathic surgery vary depending on both the skeletal pattern and specific parameters evaluated. In a study with 87 cases, Zhong et al. reported that the Smile Index and buccal corridor ratio increased in patients with Class II and that in patients with Class III, the Smile Index increased whereas the buccal corridor ratio decreased [1]. Similarly, in patients with skeletal Class III evaluated by Chiang et al., multiple parameters, including the interlabial gap, Smile Index, buccal corridors, and lip area, underwent significant postoperative changes [14]. These studies support the premise that

instead of a uniform "postoperative smile improvement" in a single direction, each parameter shows divergent responses based on the combination of skeletal pattern, dental display, and interlabial gap.

In contrast, Yang et al. investigated the association between the BCAR and facial soft tissue vertical length, maxillary incisor exposure, and crown width in a single-point posed smile [10]. A key characteristic of the present study is that we extended this area-based ratio concept to pre-to-postoperative changes, and explored both skeletal and smile-related soft tissue changes within the same regression model. However, while Yang et al. evaluated inter-individual (cross-sectional) variations, our study focused on intra-individual (longitudinal) changes. As cross-sectional inter-individual associations are not fundamentally identical to longitudinal intra-individual associations, direct comparisons of consistency or inconsistency with previous reports must be made with caution.

Furthermore, recent 3D and 4D facial imaging studies have highlighted critical information that cannot be captured by 2D static images [4,18]. 3D stereophotogrammetry has been used to quantify surface soft tissue changes of the frontal face, whereas 4D imaging has facilitated analysis of maximum displacement, kinetic trajectory, velocity, and bilateral asymmetry throughout dynamic facial expressions [15]. Age- and sex-specific 3D expression templates have also been proposed, suggesting that the reference standards for expressive movements can vary depending on age and sex [19]. Although the 2D area ratio evaluated in this study is highly feasible and can be easily implemented in routine clinical practice, future investigations are necessary to validate its correlation and compatibility with 3D and 4D datasets.

Clinical implications

First, the primary clinical implication of this study is that the postoperative smile cannot be adequately evaluated solely using lateral cephalometric parameters like the ANB angle, SNA, or SNB. Even if the skeletal treatment goals are successfully achieved, the patient's smile appearance varies depending on smile width, interlabial gap, range of maxillary dental display, and dynamic symmetry of perioral movement. Therefore, we recommend that a standardized frontal posed smile photograph be incorporated as an independent diagnostic record in preoperative diagnosis and postoperative evaluation [1], in addition to the traditional resting frontal and profile views. In clinical assessments, instead of relying on BCAR alone, clinicians should evaluate a comprehensive set of parameters, including smile width, interlabial gap, Smile Index, last visible teeth, gingival exposure, smile arc, and bilateral perioral symmetry, as a unified diagnostic panel.

Second, in preoperative counseling, clinicians must convey to patients that surgical skeletal relocation does not uniformly change the smile in a single predictable direction. In particular, the direction of change in identical parameters can differ between the Class II and Class III skeletal patterns [1]. When smile esthetics are designated as a treatment goal, smile-related soft tissue prediction is necessary in addition to hard tissue simulation [3]. However, the regression equations developed in this study are currently not at a stage suitable for individual patient prediction because of potential optimistic bias in sample estimation [20]. Currently, the BCAR is more appropriate as a clinical audit metric for documenting preoperative issues based on standardized records and re-evaluating them under identical conditions postoperatively.

Third, statistically significant and clinically meaningful changes for the patient must be clearly distinguished. Even if the morphological changes in the buccal corridors are small, the overall esthetic impression can be altered when combined with other facial elements such as gingival exposure, smile arc, and perioral symmetry. Conversely, even if the BCAR exhibits a statistically significant change, patients may not necessarily perceive this difference [6,7]. Future research should thus combine objective morphometric investigations with patient-reported outcomes (PROs) and assessments by laypersons and dental professionals to investigate the minimal clinically important difference (MCID) or clinical perception thresholds of buccal corridors.

Strengths and limitations

This study has four strengths. First, the buccal corridors were evaluated not as simple linear widths, but as an area ratio standardized by the TSA, namely, the BCAR. Second, utilizing pre-to-postoperative changes in an identical patient cohort, we explored and comprehensively investigated the factors associated with skeletal, dental, and smile-related soft tissue parameters. Third, we rigorously evaluated the intra-examiner reproducibility of the primary outcome measures using standardized clinical photography and duplicate measurements. Fourth, this study has clinical significance as it focuses on factors that can explain individual variations in BCAR changes, rather than merely reporting group-mean pre-to-postoperative differences. These findings provide fundamental insights for expanding the evaluation of post-orthognathic surgical smiles from a traditional skeletal-centric assessment to an integrated evaluation that incorporates smile-related soft tissue factors.

Nonetheless, this study has several critical limitations that govern the interpretation of our findings. First, this was a single-center, retrospective study with a sample size of 27 patients. Given the limited volume of information relative to the number of candidate variables, the stepwise regression method is highly susceptible to capturing sample-specific random variations, leading to overestimation of regression coefficients, underestimation of P values, and instability in variable selection [20]. Bootstrap internal

validation was not performed in this study; therefore, the magnitude of optimism in the reported model fit remains unknown. The reported R^2 and adjusted R^2 describe apparent fit in the study sample and should not be interpreted as validated predictive performance. A priori sample size determination based on the anticipated explanatory power and the number of candidate parameters, along with both internal and external validation, is required for establishing this model as a clinical prediction model [21]. Second, although numerous candidate variables were evaluated in the univariable analysis, no multiplicity adjustment was performed. Using $p < 0.05$ for candidate selection can introduce false-positive variables into the model, compromising the reproducibility of the identified associations. An additional fixed model incorporating baseline BCAR and a restricted set of explanatory variables was examined; however, it was specified after the primary results were available and analyzed the same small cohort. It therefore does not eliminate potential bias associated with the original significance-based screening and stepwise selection or the risk of overfitting. No FDR adjustment was performed, and the p-values remain exploratory. Third, regarding the exclusion of one patient, this decision followed our objective exclusion criteria based on the technical limitations in anatomical measurement. Specifically, a large alveolar bone defect resulting from bilateral maxillary central incisor extractions hindered reliable identification of point A on both lateral cephalometric and CBCT images, precluding reliable measurements of SNA and CBCT-derived ANB. However, this single exclusion might have influenced our estimates, and the robustness of our findings should thus be verified in future studies with larger sample sizes and sensitivity analyses.

Fourth, our patient population was heterogeneous, comprising skeletal Class II and Class III patterns, single-jaw and bimaxillary surgeries, with uneven sex and age distributions. As we did not adjust for the actual magnitudes of maxillary and mandibular displacement, occlusal plane rotation, yaw, roll, dental arch width, tooth extraction, postoperative orthodontic treatment, and auxiliary soft tissue procedures, substantial residual confounding may exist. Fifth, although analyzing change scores (Δ-variables) evaluates intra-individual changes, measurement errors accumulate from both T0 and T1 assessments. A sensitivity analysis incorporating baseline BCAR was performed, and the associations involving ΔSmile Index and ΔANB were retained. However, this finding does not establish that baseline dependency is absent or that regression to the mean and measurement error have been fully addressed. The small sample and remaining unmeasured confounding constrain interpretation, and further evaluation in larger independent cohorts is required. Sixth, 2D frontal photographs do not capture depth or the temporal trajectory of smile expressions. Perspective divergence and variations in dental arch depth may introduce projection errors because the anterior teeth, posterior teeth, and oral commissures lie at different distances from the camera. Calibration using the maxillary central incisor crown width does not fully correct these depth-dependent differences in projected magnification. Consequently, the projected visibility of posterior teeth and the measured boundaries of the buccal corridors may vary with arch depth and jaw position. Although area-based ratios reduce the influence of uniform photographic magnification, projection effects may affect BCA and TSA differently and therefore may not cancel in BCAR. Head position, lighting, smile intensity, and manual contour tracing may also introduce measurement variability. These potential errors cannot be completely excluded despite standardized photography, and their magnitude and direction were not quantified in this study. Seventh, the postoperative evaluation was performed at a mean of approximately six months. Although this interval is sufficient for edema resolution, it does not capture long-term scar tissue maturation, neuromuscular adaptation, ongoing postoperative orthodontic treatment, or long-term age-related changes in the perioral soft tissues. Eighth, this study was strictly a morphometric investigation and did not incorporate patient-reported satisfaction or third-party subjective esthetic evaluation. Consequently, the clinical significance of the observed BCAR changes cannot be directly determined.

Future research

In future research, given prior findings that the direction of BCAR change varies depending on the skeletal pattern, pre-specified stratification for skeletal Class II, Class III, and facial asymmetry is required. The primary independent variables should be pre-specified and restricted to the 3D (anteroposterior, vertical, and transverse) displacement of the maxilla, occlusal plane pitch, roll, and yaw, dental arch width, the last visible posterior teeth, smile width, and interlabial gap. The required sample size should be determined a priori based on the number of candidate parameters, expected R^2, and allowable shrinkage, and we recommend utilizing clinical hypothesis-driven restricted models or regularization methods rather than automated stepwise selection. For internal validation, bootstrapping should be employed to correct for optimism in the regression coefficients, and calibration plots should be presented. Regarding image evaluation, while preserving the clinical feasibility of standardized 2D photography, incorporating 3D stereophotogrammetry or 4D video stereophotogrammetry is highly desirable for integrating resting morphology, maximum smile expression, kinetic trajectory, and bilateral symmetry. Furthermore, mapping these objective morphometric parameters with patient-reported outcomes (PROs) and subjective esthetic evaluations by laypersons and orthodontists will advance this research from identifying statistical associations to defining clinically meaningful changes. The present study represents an exploratory stage that proposes candidate parameters for this purpose; thus, the ΔSmile Index and ΔANB should not be regarded as definitive predictors, but rather as hypotheses to be rigorously verified.

Conclusions

In this exploratory cohort, ΔSmile Index and ΔANB were statistically associated with ΔBCAR, and the fitted regression model accounted for 51.9% of the observed variance. The directions and statistical significance of

these associations were retained in an exploratory sensitivity analysis adjusting for baseline BCAR, ΔLTRW, and ΔFMA. However, the additional analyses showed that changes in TSA were closely related to changes in the interlabial gap. The association between ΔSmile Index and ΔBCAR may therefore partly reflect changes in vertical smile opening that influence both indices, including through the denominator of BCAR, rather than an independent biological relationship. The contribution of this geometric relationship could not be quantified. Given the small sample size and heterogeneity of the cohort, these findings should be interpreted as hypothesis-generating and require validation in larger independent samples.

Additional Information

Author Contributions

All authors have reviewed the final version to be published and agreed to be accountable for all aspects of the work.

Concept and design: Fumi Nakamura, Masahiro Takahashi, Rumi Matsumoto, Tetsutaro Yamaguchi

Acquisition, analysis, or interpretation of data: Fumi Nakamura, Shinya Fuchida, Masahiro Takahashi

Drafting of the manuscript: Fumi Nakamura

Critical review of the manuscript for important intellectual content: Shinya Fuchida, Masahiro Takahashi, Rumi Matsumoto, Tetsutaro Yamaguchi

Supervision: Tetsutaro Yamaguchi

Disclosures

Human subjects: Informed consent for treatment and open access publication was obtained or waived by all participants in this study. The Kanagawa Dental University Research Ethics Review Committee issued approval 1087 (initial approval, dated March 26, 2025) and 1234 (amendment approval, dated September 17, 2026). **Animal subjects:** All authors have confirmed that this study did not involve animal subjects or tissue. **Conflicts of interest:** In compliance with the ICMJE uniform disclosure form, all authors declare the following: **Payment/services info:** All authors have declared that no financial support was received from any organization for the submitted work. **Financial relationships:** All authors have declared that they have no financial relationships at present or within the previous three years with any organizations that might have an interest in the submitted work. **Other relationships:** All authors have declared that there are no other relationships or activities that could appear to have influenced the submitted work.

Acknowledgements

During the preparation of this manuscript, the authors used Gemini (Google LLC) and ChatGPT (OpenAI) for language editing, proofreading, and improving the readability and clarity of the manuscript. Following the use of these tools, the authors reviewed and revised all content as necessary and take full responsibility for the final content of the manuscript.

References

1. Zhong B, Zhou G, Yang Y, et al.: Improvement of smile characteristics in dentofacial deformity patients following orthognathic surgery. J Craniomaxillofac Surg. 2025, 53:271-8. 10.1016/j.jcms.2024.12.007
2. Cheng HC, Cheng PC: Factors affecting smile esthetics in adults with different types of anterior overjet malocclusion. Korean J Orthod. 2017, 47:31-8. 10.4041/kjod.2017.47.1.31
3. Maganzini AL, Schroetter SB, Freeman K: Improvement in smile esthetics following orthodontic treatment: a retrospective study utilizing standardized smile analysis. Angle Orthod. 2014, 84:492-9. 10.2319/072913-564.1
4. Choi JW, Lee JY, Oh TS, Kwon SM, Yang SJ, Koh KS: Frontal soft tissue analysis using a 3 dimensional camera following two-jaw rotational orthognathic surgery in skeletal class III patients. J Craniomaxillofac Surg. 2014, 42:220-6. 10.1016/j.jcms.2013.05.004
5. Xue Z, Wu L, Qiu T, Li Z, Wang X, Liu X: Three-dimensional dynamic analysis of the facial movement symmetry of skeletal class III patients with facial asymmetry. J Oral Maxillofac Surg. 2020, 78:267-74. 10.1016/j.joms.2019.09.007
6. Ioi H, Nakata S, Counts AL: Effects of buccal corridors on smile esthetics in Japanese . Angle Orthod. 2009, 79:628-33. 10.2319/080708-410.1
7. Ioi H, Kang S, Shimomura T, Kim SS, Park SB, Son WS, Takahashi I: Effects of buccal corridors on smile esthetics in Japanese and Korean orthodontists and orthodontic patients. Am J Orthod Dentofacial Orthop. 2012, 142:459-65. 10.1016/j.ajodo.2012.05.011
8. Öz AA, Akdeniz BS, Canlı E, Çelik S: Smile attractiveness: differences among the perceptions of dental professionals and laypersons. Turk J Orthod. 2017, 30:50-5. 10.5152/TurkJOrthod.2017.17021
9. Parrini S, Rossini G, Castroflorio T, Fortini A, Deregibus A, Debernardi C: Laypeople's perceptions of frontal smile esthetics: a systematic review. Am J Orthod Dentofacial Orthop. 2016, 150:740-50. 10.1016/j.ajodo.2016.06.022

10. Yang IH, Nahm DS, Baek SH: Which hard and soft tissue factors relate with the amount of buccal corridor space during smiling?. Angle Orthod. 2008, 78:5-11. 10.2319/120906-502.1
11. Wang S, Lin H, Yang Y, et al.: Use of autonomous maximal smile to evaluate dental and gingival exposure. Korean J Orthod. 2018, 48:182-8. 10.4041/kjod.2018.48.3.182
12. Van Der Geld P, Oosterveld P, Berge SJ, Kuijpers-Jagtman AM: Tooth display and lip position during spontaneous and posed smiling in adults. Acta Odontol Scand. 2008, 66:207-13. 10.1080/00016350802060617
13. Dilaver E, Suzen M, Uckan S: Evaluation of parameters related with upper lip aesthetics and dynamic smile following Le Fort I osteotomy. J Stomatol Oral Maxillofac Surg. 2022, 123:566-71. 10.1016/j.jormas.2022.05.014
14. Chiang PC, Hsin-Chung Cheng J, De-Shing Chen D, Hsu CC, Cruz Moreira RA, Chou MY: Changes in smile parameters after surgical-orthodontic treatment for skeletal Class III malocclusion. J Dent Sci. 2024, 19:1477-85. 10.1016/j.jds.2024.02.021
15. Quast A, Sadlonova M, Asendorf T, et al.: The impact of orthodontic-surgical treatment on facial expressions-a four-dimensional clinical trial. Clin Oral Investig. 2023, 27:5841-51. 10.1007/s00784-023-05195-9
16. von Elm E, Altman DG, Egger M, Pocock SJ, Gøtzsche PC, Vandenbroucke JP: Strengthening the Reporting of Observational Studies in Epidemiology (STROBE) statement: guidelines for reporting observational studies. BMJ. 2007, 335:806-8. 10.1136/bmj.39335.541782.AD
17. Koo TK, Li MY: A guideline of selecting and reporting intraclass correlation coefficients for reliability research. J Chiropr Med. 2016, 15:155-63. 10.1016/j.jcm.2016.02.012
18. Enez A, Altıparmak N, Akdeniz BS, Akdeniz SS: 3D analysis of smile transformation in patients with class III deformities following orthognathic surgery: a stereophotogrammetric study. Clin Oral Investig. 2026, 30:57. 10.1007/s00784-026-06748-4
19. Schutte H, Muradin MS, Bielevelt F, Ten Harkel TC, Speksnijder CM, Rosenberg AJ: Creating three-dimensional templates of smiling and pouting faces for different sex- and age groups. J Clin Med. 2022, 11:7257. 10.3390/jcm11247257
20. Babyak MA: What you see may not be what you get: a brief, nontechnical introduction to overfitting in regression-type models. Psychosom Med. 2004, 66:411-21. 10.1097/00006842-200405000-00021
21. Riley RD, Snell KI, Ensor J, Burke DL, Harrell FE Jr, Moons KG, Collins GS: Minimum sample size for developing a multivariable prediction model: part I - Continuous outcomes. Stat Med. 2019, 38:1262-75. 10.1002/sim.7993